CONF-9609994--9   SAND96-2401C
SAND--96-2401C

FINITE-ELEMENT MODELING OF NANOINDENTATION FOR DETERMINING THE MECHANICAL PROPERTIES OF IMPLANTED LAYERS AND THIN FILMS[*]

J. A. Knapp, D. M. Follstaedt, J. C. Barbour and S. M. Myers

Sandia National Laboratories

Albuquerque, New Mexico 87185

RECEIVED
OCT 15 1996
OSTI

Abstract

The mechanical properties of implanted layers and thin films on dissimilar substrates are difficult to accurately determine. Nanoindentation of the layer provides information, but detailed numerical modeling is required in order to separate the properties of the layer from those of the substrate. We describe here the procedures we have developed to accomplish this modeling with the commercially available finite-element code ABAQUS. Using these techniques, we are able to extract from nanoindentation testing the yield stress, Young's modulus, and hardness of the layer material, with an absolute accuracy of at least 20%. The procedure is applicable to layers as thin as 50 nm on essentially any substrate, hard or soft. We have used it for materials ranging from ion-implanted layers to thin films of metals and dielectrics formed using plasma-deposition methods. An example is given of O-implanted Al, a thin, hard layer on a soft substrate.

Send proofs and correspondence to:

J. A. Knapp
MS 1056
Sandia National Laboratories
Albuquerque, New Mexico, USA 87185-1056
phone: 1-505-844-2305
fax: 1-505-844-7775
email: jaknapp@sandia.gov

MASTER

DISCLAIMER

Introduction

As many papers in this proceedings attest, ion implantation and various ion-assisted depositions are used extensively to form materials with improved hardness, wear and corrosion properties. In order to characterize the mechanical properties of thin films and surfaces from these types of ion-beam processes, nanoindentation tests are often performed to extract the hardness and elasticity. In nanoindentation, a diamond tip is pushed into the material under very fine control and the reaction force is measured as a function of depth. The force required to indent to a given depth provides a measure of the hardness of the material, while the recovery of the material during withdrawal indicates the elasticity. For bulk samples, the hardness and Young's modulus of the material can be extracted directly from the data.[1] However, for thin film samples, especially when the layer has a thickness only a few times the maximum depth of the indent, the observed load vs. force response is a combination of the mechanical response of the layer and that of the substrate. This combined response must be modeled in order to separate the contribution of the surface layer properties from those of the known substrate. The non-linear nature of the problem requires finite-element numerical modeling. The methodology described in this paper uses a commercial finite-element code, and thus can be transferred to other laboratories. We have been using the technique on a wide variety of materials and believe it to be applicable to essentially any thin film study where mechanical properties are of interest.

Modeling

For numerical modeling we use the large-strain, finite-element code ABAQUS.[2] There are two versions (solvers) presently available: Standard, optimized for static problems where inertia or time-dependent properties are not important, and Explicit, a solver best used for dynamic calculations with significant kinetic energy in the model. A third solver was also used extensively, a beta-version conjugate gradient solver which was to be released as part of ABAQUS/Explicit. Because this solver is no longer supported, we now use ABAQUS/Standard for most of our calculations. All of these solvers allow modeling friction and the changing contact between indenter tip and layer surface, with certain restrictions in Standard on how far the surfaces can slide relative to one another. The solvers also allow the input of pre-existing stress in the layers and can be used for either 2 or 3 dimensional calculations. The results obtained from all three solvers were compared for selected problems, and except for computation time, the outputs have been identical. This reproducibility between solvers, along with success at

modeling indentation of known bulk samples, assures us that the numerical evaluations are accurate. Table I shows typical run times for the three solvers. (The Explicit dynamic solver can be used for these quasi-static problems by increasing the model pin velocity as much as possible while still keeping the kinetic energy low relative to total energy). For 2-dimensional simulations, the Standard solver is the best choice, while the conjugate gradient solver is most efficient for the larger 3-dimensional simulations.

For each sample to be studied, we generate either a 2-dimensional, axisymmetric mesh or a full 3-dimensional mesh specific to the sample structure and the tip shape.[3] For an example mesh, see Fig. 1. The tip shape (area as a function of depth into the samples, including tip rounding) is calibrated by Nano Instruments[4] using indents of a silica sample with known mechanical response. A 2-dimensional mesh uses cylindrical symmetry and models the pin as a cone modified by the area vs. depth function, while a 3D mesh models it with the actual 3-sided pyramidal shape, corrected for tip rounding. It is only necessary in 3 dimensions to model a 60° section of the pin and sample because of symmetry. The size of the meshes is generally 6-8 μm deep by 6-8 μm radius, which is large enough to avoid edge effects. Comparison of results using the 2D and 3D models shows very little difference and thus for most cases the 2D simulations are all that are required.

Layer thickness and composition are pre-determined by a technique such as Rutherford backscattering spectrometry (RBS). Density, Poisson's ratio and a known stress-strain curve are specified for the diamond tip and the substrate, and then a series of simulations with different values of the surface material's properties are performed until a suitable fit is obtained to the experimental force vs. depth curve. The modeling uses the layer density assumed in RBS analysis or measured by other techniques. Generally only the yield stress Y (defined at a plastic strain of .002) and Young's modulus E are varied, with the hardening rate fixed at a typical value for the material. The initial stress in the layer (tensile or compressive) can also be input, if known.

The finite-element analysis to determine Y and E is an iterative technique, so a procedure was developed to minimize the number of runs required to find the material properties giving a good fit to the experimental response.[3] This procedure is based on parameterizing the indentation response curves, both experimental and simulated. Since the loading portion of each indentation response curve is sensitive to both Y and E, while the unloading portion is determined largely by E, one characteristic parameter for each portion of the curve is sufficient.

We chose the loading force at a fixed depth (such as at 80% of maximum depth) as the first parameter and the initial unloading slope as the second.

The procedure is as follows: (1) a series of 4-5 simulations are run with values of Y and E selected to approximately bracket the expected experimental values. (2) The loading forces F_L and unloading slopes S_U of the experimental and simulated force vs. depth curves are extracted by curve-fitting. (3) A four-parameter linear regression using only the simulation values is performed, giving one equation for Y and one for E, each as a linear function of both F_L and S_U. (4) The experimental points are averaged, giving an average F_L and S_U for the experiment. (5) The average values of F_L and S_U from the experiment are used in the equations to derive the Y and E which should, when used in a simulation, give a response curve that matches the "average" experimental curve. These steps give the projected best values of Y and E, as well as error bounds on Y and E based on both the spread in the experimental results and the quality of the linear regression fit. (6) Finally, one or two additional simulations are performed to confirm that the interpolated values give a good fit to experiment.

An assumption made in the procedure above is that the dependence of F_L and S_U on Y and E is linear, but we have found this to be a good approximation when the bracketing values for Y and E are reasonably close to the final values. The value of this procedure lies both in providing a good fit in a minimum of calculations and in quantifying the error bars for the final values of Y and E.

Since the hardness H (~3 times Y for ductile materials) is more commonly used than Y for a figure of merit, we also use the simulations to evaluate H for the layer material. Of course, the apparent hardness of the simulated sample is available at any point in a calculation by dividing the indentation force by the area of contact. However, this is a hardness representing the combined properties of the layer and substrate. To evaluate H for the layer material alone, we do an additional simulation using the Y and E derived above and the other properties of the layer for the material in both layer and substrate. That is, we do an indentation in the computer of a hypothetical "bulk" sample of the layer material and use the results of that calculation to determine H.

Example

Figure 2 shows several experimental nanoindentation curves from an O-implanted Al sample, along with the best-fit modeling simulation. The alloy layer at the surface of this sample

contains 10 at.% O to a depth of ~390 nm, and is composed of a fine dispersion of 0.8-1.6 nm diameter γ-Al_2O_3 precipitates in the Al matrix. The sample is part of our program investigating implantation and plasma-based synthesis methods for forming new alloys of aluminum with very high strength.[5-11] It was formed by a series of O implants at energies ranging from 200 keV down to 25 keV, with the fluences tailored to give a uniform O concentration over a depth of 400-500 nm.[11] The fine dispersion of very small precipitates substantially hardens the Al in the implanted layer, as has been discussed elsewhere.[5,8] This specimen is a good test for illustrating the application of our modeling, since the very hard layer on the soft Al substrate is a difficult combination for nanoindentation without modeling.

For each experimental measurement, the pin was inserted to 150 nm, held at constant load for 15 seconds, and then withdrawn. During the hold segments the sample relaxes somewhat through creep, allowing the indenter to push in to greater depths; this is reflected by the horizontal sections in the experimental curves near 150 nm. The apparent hardness of the sample is indicated by the required force during the loading portion of the curve, while the elastic properties are reflected in the slope of the curve during the unloading segment. The change in slope near 60 nm is immediate evidence of the influence of the soft substrate. A series of 10 indents were performed, spaced 15 μm apart; only three are shown in the figure for clarity.

The diamond indenter and Al substrate were modeled using published parameters, with the response of the diamond being purely elastic. The Al(O) layer was modeled as an elastic-plastic solid, using the metal plasticity model in ABAQUS with a Mises yield surface and associated plastic flow.[12] Poisson's ratio for pure Al (0.347) was used, and the work hardening rate was fixed for all simulations at 1.5 GPa, a value which appears from the literature to be typical of most Al alloys and Al with impurities.[13] The pre-existing stress was assumed to be negligible for the layer. The implanted layer depth distribution was modeled using three layers, thicknesses 340, 50 and 50 nm, with the mechanical properties of each layer linearly scaled at 100, 70 and 30% of the nominal values for 10 at.% O. The two 50 nm layers model the transition between the implanted layer and the pure Al substrate. The center portion of the 2D mesh is shown in Fig. 1.

Using the procedure described above, interpolation of simulation results predicted a best fit to the data using Y = 2.4 ± 0.13 GPa and E = 134 ± 7 GPa for the Al(O) layer. A simulation using these values is shown as the solid line in Fig. 2. Except for the short flat sections in the experiment at 160 nm due to creep, the match is quite good. Creep is a time-dependent material property, and as such is not modeled. Once the best values for Y and E are found, the simulation

using those values provides a wealth of other information such as the progression and extent of plastic flow or the magnitude of stress in various parts of the sample structure. ABAQUS can provide plots or tables of essentially any relevant mechanical property of the sample at any point during the indent. Such information can be useful in understanding the experimental results. Figure 3 shows plots of the plastic flow for the simulation in Fig. 2 for three different tip penetration depths, demonstrating that the substrate is already yielding substantially at an indentation depth of 41 nm, even though only about 1/2 of the hard implanted layer beneath the contact point has yielded. By the time the indenter has reached 106 nm, the flow in the substrate has extended to a radius 4 times the contact radius. This plastic flow in the substrate is the reason for the change in slope in the loading curve near 50-60 nm. At the deepest indentation, 162 nm, the plastic zone in the substrate extends 3.5 μm deep and to a radius of 2.4 μm.

The apparent hardness of the sample is just the force on the pin divided by the area of contact, which can be obtained from a plot of the deformed mesh. Figure 4 shows a plot of the combined hardness given by the simulation of Fig. 2 as a function of depth during the indent. As expected, the hardness starts out high, since the pin is barely penetrating the layer, then becomes lower as the substrate starts to yield. This is another indication that the very hard layer on a soft substrate is a difficult sample to measure without modeling. As described above, we also derived the hardness for the layer alone by doing an additional simulation using the layer Y and E and other properties throughout the simulated sample. This value, H = 7.5 ± 0.4 GPa, is indicated on Fig. 4 along with the hardness of the Al substrate.

Conclusions

The use of finite-element simulations can substantially increase the information derived from nanoindentation testing of thin layers and can help provide insight into sample behavior during the experiment. Using the procedures outlined here, an experimenter can determine E, Y, and H for a thin layer on an arbitrary substrate, along with associated error bars for each quantity. Some uncertainties remain. The effect of creep cannot be modeled at present. Residual stress in thin films is known to affect their indentation response[14]; although we can include residual stress in the model, the value is often unknown. For deposited layers the strength of bonding between layer and substrate is also unknown; we assume a perfectly bonded interface. Finally, the precise shape of the tip, particularly at these shallow indents, may not be sufficiently well

known. However, even with all these modeling uncertainties considered, we judge the absolute uncertainty in our results to be no more than 20 %.

Acknowledgments

References

[1] W. C. Oliver and G. M. Pharr, J. Mater. Res. 7 (1992) 1564.

[2] ABAQUS, Hibbitt, Karlsson & Sorensen, Inc., Pawtucket, RI.

[3] J. A. Knapp and D. M. Follstaedt, Mat. Res. Soc. Symp. Proc., (1996) in press.

[4] Nanoindentation tests were performed at Nano Instruments, Inc., Knoxville, TN.

[5] D. M. Follstaedt, J. A. Knapp, J. C. Barbour, S. M. Myers and M. T. Dugger, Proc. of the Int. Conf. on Beam Processing of Advanced Materials, 10/30-11/2/95, (1996) 77.

[6] J. A. Knapp, D. M. Follstaedt, and S. M. Myers, J. Appl. Phys. 79 (1996) 1116.

[7] J. C. Barbour, D. M. Follstaedt, and S. M. Myers, Nucl. Instr. & Meth. B106 (1995) 84 .

[8] R. J. Bourcier, S. M. Myers and D. H. Polonis, Nucl. Instr. & Meth. B44 (1990) 278.

[9] R. J. Bourcier, D. M. Follstaedt, M. T. Dugger and S. M. Myers, Nucl. Instr. & Meth. B59/60 (1991) 905.

[10] D. M. Follstaedt, S. M. Myers and R. J. Bourcier, Nucl. Instr. & Meth. B59/60 (1991) 909.

[11] D. M. Follstaedt, S. M. Myers, R. J. Bourcier and M. T. Dugger, Proc. of the Int. Conf. on Beam Processing of Advanced Materials, 11/2-5/92, (TMS, Warrendale, PA, 1993) 507.

[12] Mechanical Behavior of Materials, eds. F. A. McClintock and A. S. Argon (Addison-Wesley, Reading, MA, 1966) pp. 276-279.

[13] Atlas of Stress-Strain Curves, Edited by H. E. Boyer (ASM International, Metals Park, Ohio, 1987) 383.

[14] G. M. Pharr, T. Y. Tsui, A. Bolshakov and W. C. Oliver, Mat. Res. Soc. Symp. Proc. 338 (1994) 127.

Table I. Comparison of run times for typical problems for three different ABAQUS solvers. Run times are for a DEC AlphaStation 250 4/266.

	2D (~3000 elements)	3D (~10,000 elements)
ABAQUS/Standard	20 min.	48 hrs.
ABAQUS/Explicit CGS*	50 min.	10 hrs.
ABAQUS/Explicit (dynamic)	8 hrs.	na

* The Explicit CGS solver is no longer supported.

Figure Captions

Figure 1. A 2-dimensional model mesh for simulating nanoindentation of the O-implanted Al sample. The implanted region is modeled by three layers 340, 50, and 50 nm thick. The substrate is modeled by two layers and the size of the layer plus substrate is 8 μm deep by 8 μm wide.

Figure 2. Nanoindentation load vs. depth response curves for a 10 at.% O-implanted Al sample. Both experimental response curves and a best-fit modeling simulation are shown.

Figure 3. A series of plots showing the boundary of plastic flow (at 0.002 strain) at three indentation depths of the simulated indent. The light gray regions have yielded.

Figure 4. Hardness derived from simulation of the nanoindentation of the O-implanted Al. The curve is hardness vs. depth for nanoindentation of the layer/substrate combination. Also indicated is the hardness found for a "bulk" piece of the layer material and the hardness for the Al substrate.
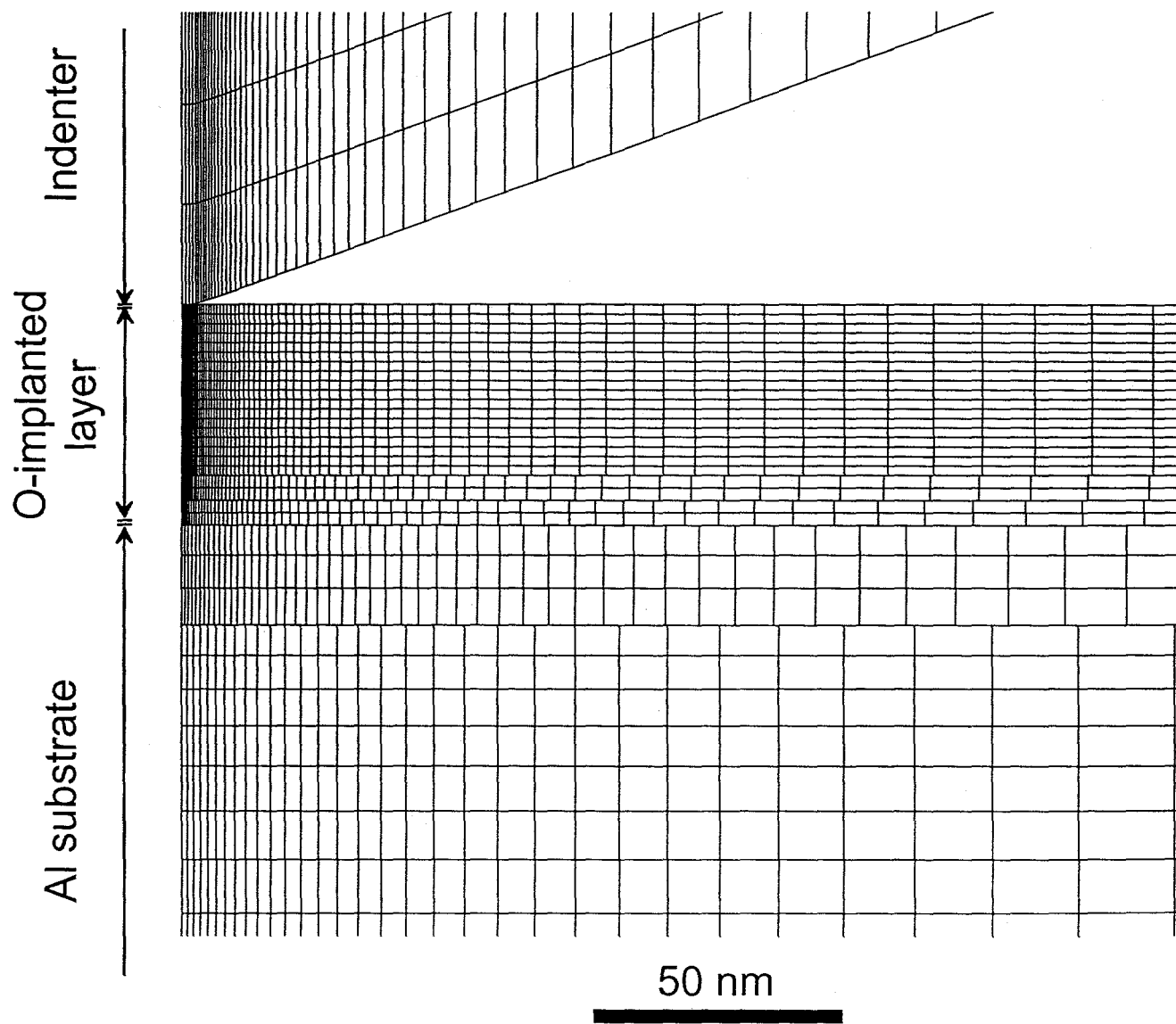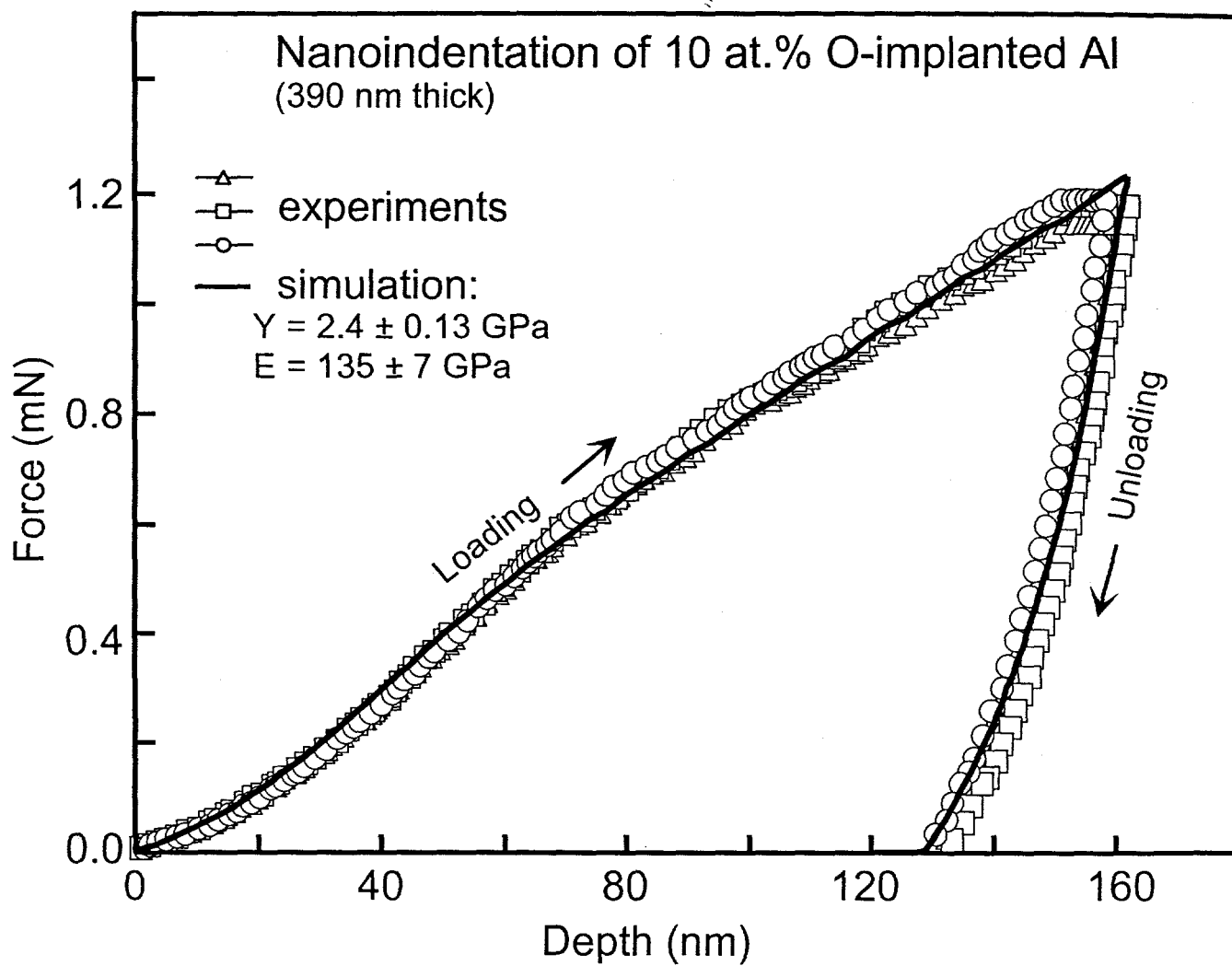
Indenter

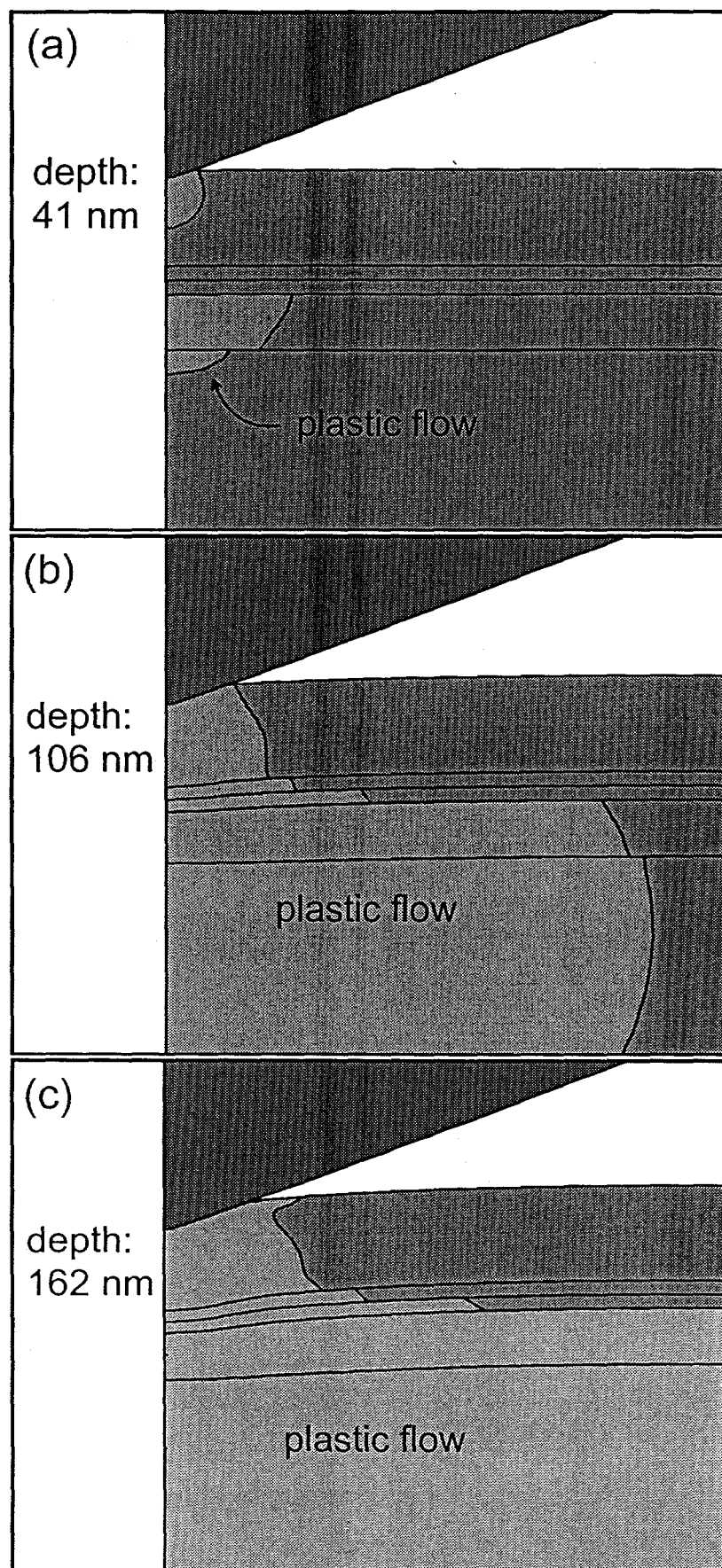O-implanted layer
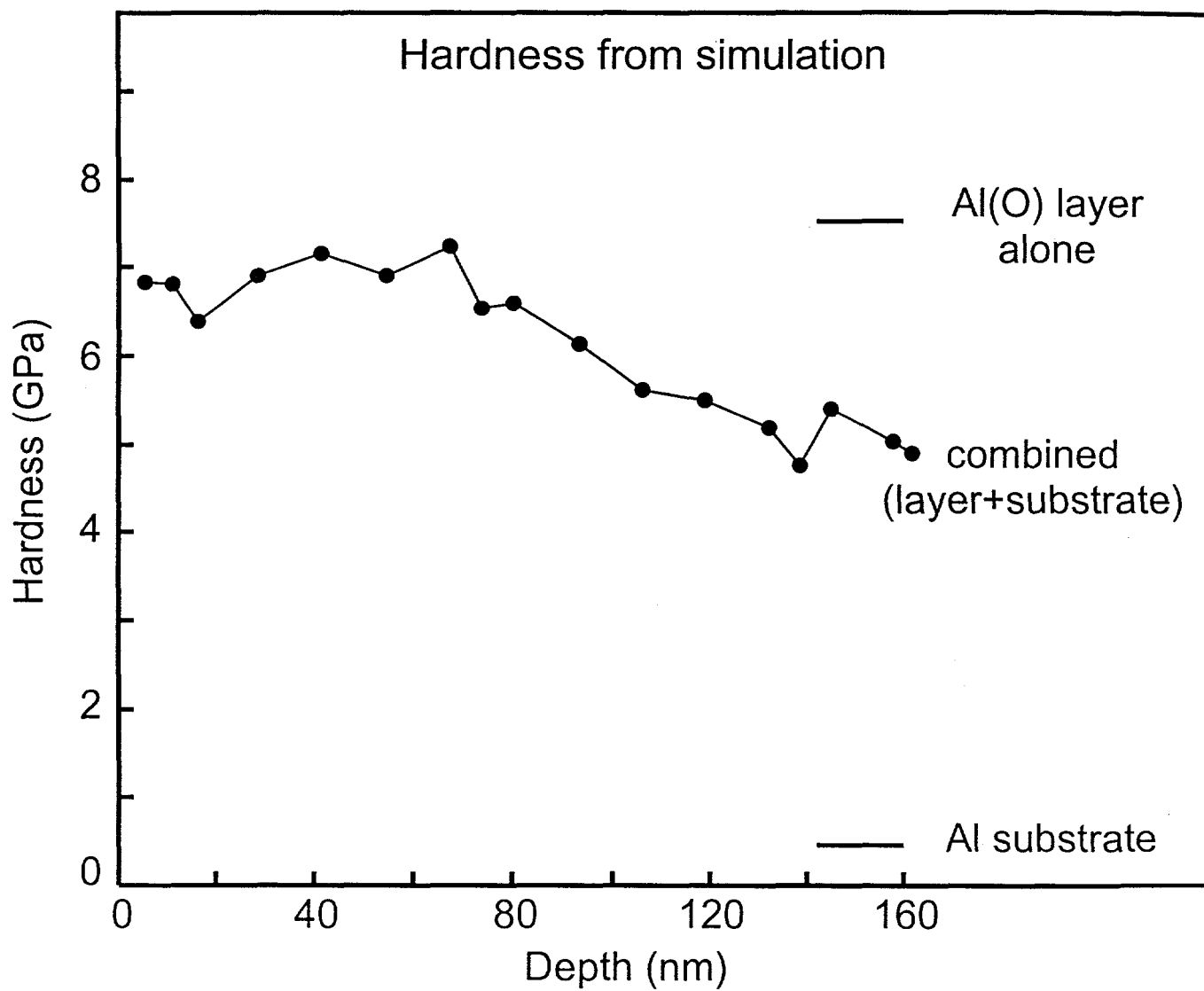
Al substrate

50 nm

Figure 1

Nanoindentation of 10 at.% O-implanted Al
(390 nm thick)

experiments

simulation:
Y = 2.4 ± 0.13 GPa
E = 135 ± 7 GPa

Loading

Unloading

Figure 2

(a) depth: 41 nm — plastic flow

(b) depth: 106 nm — plastic flow

(c) depth: 162 nm — plastic flow

Figure 3

Figure 4